JOURNAL OF MATERIALS SCIENCE 30 (1995) 2305–2312

Subcritical interlaminar crack growth in fibre composites exhibiting a rising *R*-curve

A. OKADA*
Scientific Research Laboratory, Nissan Motor Co., Ltd, 1, Natsushima-cho, Yokosuka 237, Japan

I. N. DYSON, A. J. KINLOCH
Department of Mechanical Engineering, Imperial College of Science, Technology and Medicine, Exhibition Road, London SW7 2BX, UK

Subcritical crack growth behaviour has been evaluated in composite laminates based on uniaxial carbon fibres in poly(ether-ether ketone) matrices. Double cantilever beam (DCB) specimens have been employed to give mode I loading and it is first shown that the materials exhibit a rising *R*-curve, i.e. the value of the interlaminar fracture energy, G_{Ic}, increases as the crack propagates through the specimens. Secondly, when a DCB specimen is held at a constant displacement, subcritical crack growth is found to occur. The velocity of the subcritical crack growth, v, has been measured using a load–relaxation technique. Hence, values of the crack velocity, v, have been obtained as a function of the strain-energy release rate, G_I, applied during subcritical crack growth. Owing to the presence of the *R*-curve, these data have been measured at various stages during the development of the *R*-curve. The relationships between v and G_I are modelled using power-law expressions. Finally, it is considered that the *R*-curve behaviour is most likely caused by the fibre bridging which develops behind the crack tip as the delamination propagates through the specimen. Fibre bridging allows stress to be transferred across the crack faces, behind the advancing crack tip, and so results in a "shielding" of the stress field at the crack tip from the applied stress. Therefore, the expression ascertained for the relationship between the velocity, v, of subcritical crack growth and the corresponding value of G_I has been further refined and modelled to account for the presence of fibre bridging.

1. Introduction

Owing to their high modulus and strength, composite laminates have been widely employed to manufacture light-weight engineering structures. However, a major problem is their relatively low interlaminar strength, which is basically governed by the properties of the polymeric matrix materials [1]. It is therefore important to improve the mechanical properties of the matrix, particularly with respect to improving the toughness of the matrix. In addition, predicting the degradation of the mechanical behaviour of the composite arising from delaminations is one of the important aspects which needs to be studied further for the safe application of composites to load-bearing structures. The initiation and propagation of interlaminar cracks are basically caused by shear and tensile stresses arising between the plies of the fibre composite. Under long-term loading conditions, subcritical, interlaminar crack growth may be caused by cyclic fatigue loads, or from the application of static loads and displacements. Therefore, such loading conditions, which are commonly encountered, can typically lead to a degradation of the mechanical properties of the composite material.

Further, in some composites, *R*-curve behaviour also needs to be taken into account when analysing the crack propagation behaviour. An "*R*-curve", or "resistance curve", describes the observation that the value of the interlaminar fracture energy, G_{Ic}, may increase as the delamination propagates through the composite. Under mode I(tensile) loading, fibre bridging has been proposed as the dominant mechanism responsible for the *R*-curve. Fibre bridging allows stress to be transferred across the crack faces, behind the advancing crack tip, and so results in a "shielding" of the stress field at the crack tip from the applied stress [2–4]. Naturally, it is considered that this shielding effect may influence the rate of subcritical crack growth [5]. Therefore, the main objective of the present study was to study polymeric fibre-composites which exhibit an *R*-curve, and thereby investigate the effect of the *R*-curve on the subcritical crack growth behaviour which has been reported under the application of

Present address: Japan Fine Ceramics Center, 4-1, Mutsuno, 2-Chome, Atsuta-ku, Nagoya, 456 Japan.

0022–2461

a constant displacement [5]. A second aim was to compare the behaviour of unidirectional carbon-fibre laminates based upon poly (ether-ether ketone) (PEEK) matrices, where the composites were either prepared from a "sheet" or "tape" type or "mixed-fibre" type prepreg.

2. Experimental procedure

2.1. Materials

The materials used in the present study were two types of carbon fibre/poly (ether-ether ketone) composite. One was prepared from unidirectional prepreg tapes of APC-2 (produced by ICI Composites Inc., USA). The APC-2 material consisted of continuous carbon-fibres of "AS-4" type (Hercules Inc., USA) in a matrix of the thermoplastic poly (ether-ether ketone). The thickness of each prepreg tape was approximately 125 μm, and the nominal fibre volume fraction was 70%. The other type of composite was a fabric type of prepreg, namely, TEXXES Hybrid Fabric CWC1013D (supplied by Nittobo Co. Ltd, Japan). This was in the form of unidirectional, continuous carbon-fibres (T300 type fibres from Toray Co. Ltd, Japan) which were interwoven, normal to the direction of the carbon fibres, with continuous fibres of poly (ether-ether ketone). The diameters of the carbon fibres and PEEK fibres were about 8 and 35 μm, respectively [6], and the fibre volume fraction was approximately 70%.

2.2. Test specimens

In order to produce the double cantilever beam (DCB) specimens for the mode I, interlaminar crack growth tests, composite sheets of 40 plies with approximate dimensions of 145 mm by 295 mm were hot-pressed, at a temperature of 380° C for the APC-2 composite and at 400° C for the TEXXES composite, according to the manufacturer's instructions. A folded aluminium foil, coated with release agent, was inserted between the central plies to produce an initial starter crack. The hot-pressed sheets of material were cut into specimens 25 mm wide and 140 mm long, with the fibres running parallel to the subsequent direction of crack growth. In order to apply the load, end blocks were made from aluminium alloy and were bonded on to the specimens. The surfaces of the composite specimens and the end blocks were prepared for bonding by using a treatment involving grit-blasting followed by wiping with a solvent-impregnated cloth. The adhesive used for adhering the end blocks was a modified epoxy (E38, supplied by Permabond, UK) and was cured at 60 °C for 1 h. The side of the specimen was painted white with typewriter correction fluid, and marked at 5 mm intervals so that the position of the crack front could be monitored during the fracture tests using a low-power optical microscope.

2.3. Fracture tests

A tensile testing machine was used for evaluating the R-curve behaviour, and the subsequent subcritical crack growth behaviour, of the composites. A test temperature of 20° C was used. Firstly, the load was applied at a constant crosshead speed of 2 mm min^{-1} and the associated load versus displacement trace was recorded, with the position of the crack being regularly marked on this trace. From these experimental data, the interlaminar fracture energy, G_{Ic}, as a function of the length of the propagating crack could be determined; i.e. the R-curve could be ascertained. Secondly, with a knowledge of the R-curve, another specimen was loaded at a constant crosshead speed of 2 mm min^{-1}, and again the crack was allowed to propagate whilst the load and displacement were recorded. However, now the crosshead was occasionally stopped and the displacement held constant. During the period the displacement was held constant, any change in the load was recorded as a function of time, and the position of the crack was again monitored using a low-power optical microscope.

It should be noted that previous work [5] has confirmed that the load relaxation, during the time period that the DCB specimen is held at a constant displacement, is not due to creep deformation of the composite. This was confirmed from a control test, where a constant displacement was applied to the composite. In this experiment one of the fractured half-beams (20 plies thick) from a DCB test was used and one end of the beam was clamped and the other end was loaded normal to the axis of the beam. No significant load relaxation was recorded.

2.4. Calculation of interlaminar fracture energies

The mode I interlaminar fracture energy, G_{Ic}, may be determined using the "corrected-displacement" beam equation [2, 3, 6, 7]

$$G_{Ic} = \frac{F}{N}\frac{3P\delta}{2B(a + \chi_I h)} \tag{1}$$

where $2h$ is the thickness of the composite specimen, B is width of the specimen, P is the applied load, δ is the displacement and a is the corresponding crack length. The term χ_I is a correction factor for root rotation, which is introduced to give an effective crack length, and the terms F and N are used to correct the effect of tilting of the end blocks and large displacements [7], such that

$$F = 1 - \frac{3}{10}\left(\frac{\delta}{a}\right)^2 - \frac{3}{2}\left(\frac{\delta l_1}{a^2}\right) \tag{2}$$

and

$$N = 1 - \left(\frac{l_2}{a}\right)^3 - \frac{9}{8}\left[1 - \left(\frac{l_2}{a}\right)^2\right] \times \left(\frac{\delta l_1}{a^2}\right) - \frac{9}{35}\left(\frac{\delta}{a}\right)^2 \tag{3}$$

where l_1 and l_2 are the distances of the load-point above the beam and half-length of the end block respectively, as shown in Fig. 1.

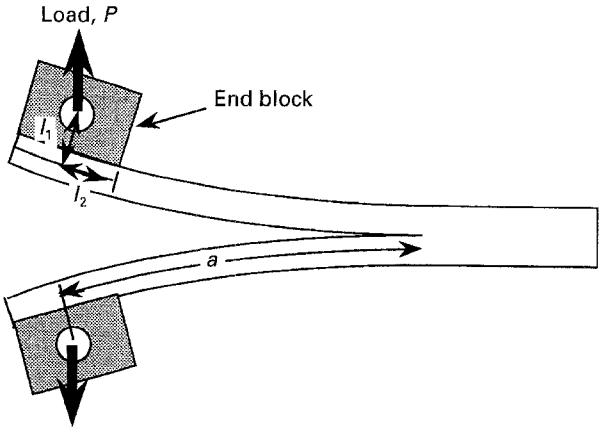

Figure 1 Schematic drawing of the double cantilever beam specimen.

For the subcritical crack growth tests, expressions for the crack velocity, v, and the corresponding G_I values are given [5] by, respectively

$$v = -\frac{h}{6}\left(\frac{\delta E_{11} B}{N}\right)^{1/3} P^{-4/3}\frac{dP}{dt} \quad (4)$$

$$G_I = \frac{3FP^{4/3}\delta^{2/3}}{N^{2/3}B^{4/3}hE_{11}^{1/3}} \quad (5)$$

where E_{11} is the axial Young's modulus. The value of Young's modulus, E_{11}, and the correction factor, χ_I, were determined from plots of $(C/N)^{1/3}$ versus a; because, based on the expression for the compliance [7]

$$\left(\frac{C}{N}\right)^{1/3} = \left(\frac{8}{Bh^3E_{11}}\right)^{1/3}(a + \chi_I h) \quad (6)$$

It should be noted that fibre bridging may cause the value of the Young's modulus obtained in this way to be somewhat greater than the true material value, as determined, for example, from independent three-point bend tests. The value of the correction factor, χ_I, for root-rotation may be also greater than that predicted theoretically [5, 6].

3. Results

Fig. 2a shows the results for the subcritical crack growth tests on the APC-2 composite, where on three occasions the crosshead of the testing machine was stopped and the displacement held constant, and the corresponding R-curve for this series of tests is shown in Fig. 2b. For these three subcritical crack growth tests (Fig. 2a) the length of the delamination, a, when the crosshead was halted was 29, 31 and 35 mm, respectively (i.e. marked as SCG1, SCG2 and SCG3 in Fig. 2b). The results are plotted in the form of the subcritical crack velocity, v, versus the strain energy release rate, G_I, applied during the course of the test. It may be seen that, for the logarithmic axes which have been employed, the relationships between v and G_I are linear. Further, for the subcritical tests conducted using the longer crack lengths (i.e. for values of a of 31 and 35 mm respectively: the SCG2 and SCG3 tests) the a versus G_I linear relationship shifts to high values of G_I, and the slope of the line decreases. The corresponding R-curve for this series of tests is shown in

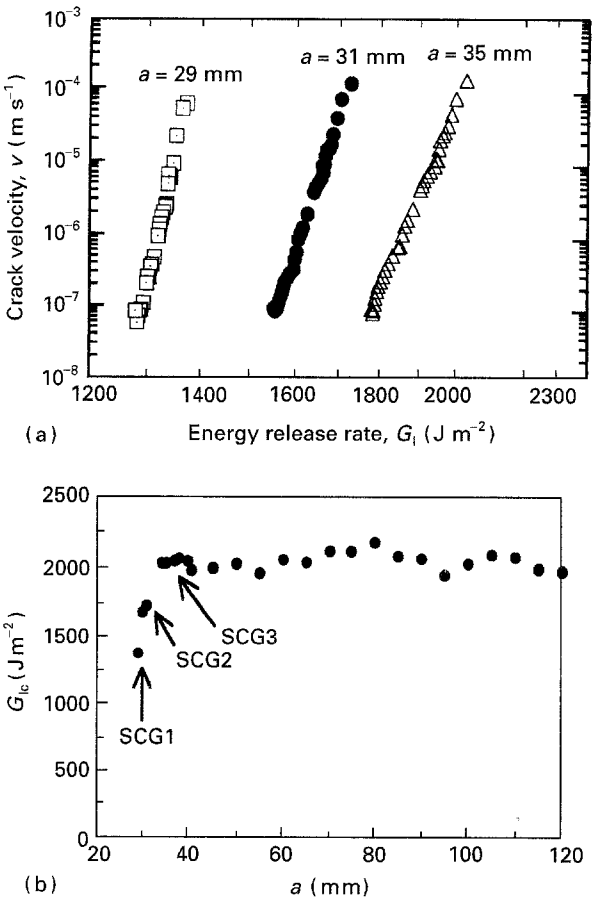

Figure 2 Results of the crack growth tests for the APC-2 unidirectional carbon-fibre/PEEK composite. (a) Subcritical crack growth velocity, v, versus G_I obtained from constant displacement tests in three regions of the R-curve. (b) The R-curve (displacement rate used was 2 mm min^{-1}).

Fig. 2b. The G_{Ic} values, at the crack lengths at 29 and 31 mm are 1375 and 1725 J m^{-2}, respectively, both of which are in the rising region of the R-curve. However, for the crack length of 35 mm, the value of G_{Ic} is 2025 J m^{-2} and this corresponds to the steady state, plateau, region of the R-curve.

Fig. 3 shows the results for the TEXXES composite material. During loading at a constant displacement rate to obtain the R-curve, this material revealed a tendency to exhibit slip–stick crack growth behaviour [6]. Hence, the subcritical crack growth experiments could only be obtained from a limited region of the G_{Ic} versus a relationship (i.e. the R-curve shown in Fig. 3b) where stable crack growth was observed. (However, during the actual subcritical crack growth experiments the crack propagation was always stable.) The first of the subcritical crack growth experiments (SCG1) was undertaken when the crack length was 29 mm, with a corresponding value of G_{Ic} of 2510 J m^{-2}, and this was in the rising region of the R-curve. The second and third tests were made in the steady-state region of the R-curve. The values of the crack length, a, were 31 and 33 mm, respectively and the corresponding values of G_{Ic} were 2790 and 2765 J m^{-2}. Because the values of G_{Ic} at the crack lengths of 31 and 33 mm are approximately the same, the relationships between a and G_I were very similar. It should be noted that, as for the APC-2 composite, the results for the TEXXES material reveal that: (i) for

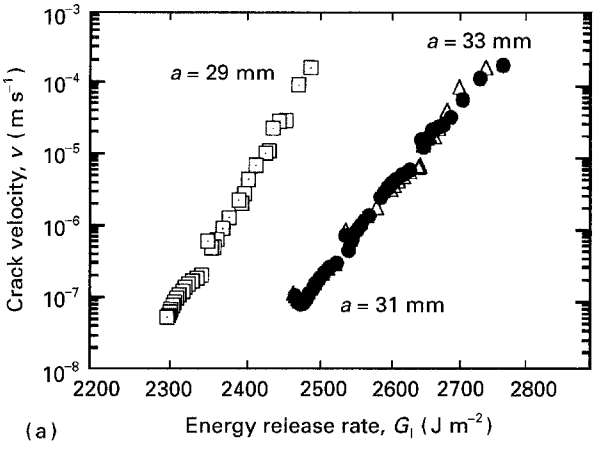

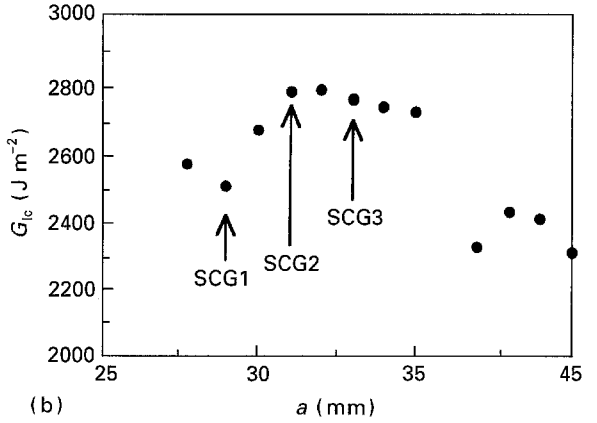

Figure 3 Results of the crack growth tests for the TEXXES unidirectional carbon-fibre/PEEK composite. (a) Subcritical crack growth velocity, v, versus G_I obtained from constant displacement tests in three regions of the R-curve. (b) The R-curve (displacement rate used was 2 mm min^{-1}).

the logarithmic axes which have been employed, the relationships between v and G_I are linear, and (ii) for the longer crack lengths of $a = 31$ and 33 mm, this linear relationship shifts to high values of G_I, and the slope of the line decreases.

Thus, the load–relaxation tests, where the displacement is held constant, give linear relationships between $\log v$ and $\log G_I$ shown in Figs 2a and 3a for the two types of poly(ether-ether ketone)-based composites. Now, these data may be empirically described by an equation of the form [8]

$$v = RG_I^m \tag{7}$$

Table I shows the values of $\log R$ and m which have been determined from the relationships shown in

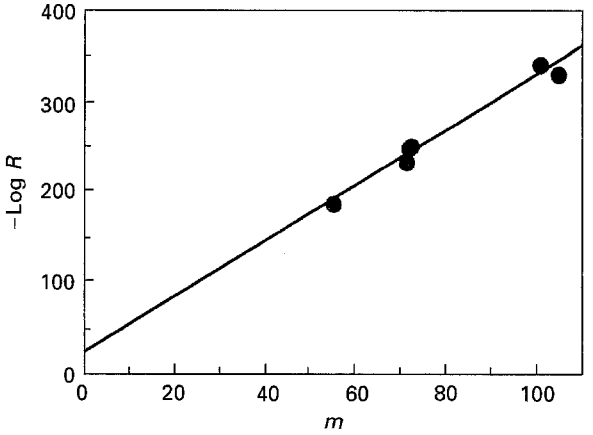

Figure 4 Relationship between the values of $-\log R$ and m for both types of composite. $-\text{Log}\,R = 20.123 + 3.1128\,m$; $R^2 = 0.972$.

Figs 2a and 3a. For the APC-2 composite, the first subcritical crack growth test (SCG1) gives the values of $m = 104.7$ and $\log R = -332.7$, the values for the second test (SCG2) at a longer crack length are $m = 71.1$ and $\log R = -233.9$, and for the third test (SCG3) at the longest crack length the values are $m = 55.4$ and $\log R = -187.1$. Thus, subcritical crack growth tests conducted in the initial rising region of the R-curve give a higher value of m and a smaller value of $\log R$, compared to tests undertaken in the later part of the rising region, or in the steady-state region. Considering the results obtained from using the TEXXES material, then the present subcritical crack growth tests give results which are similar to those obtained from the APC-2 composite. The first test (SCG1) gives the values of $m = 100.3$ and $\log R = -344.3$. The other two tests (SCG2 and SCG3) were in the steady-state region of the R-curve and resulted in the values of $m = 72.4$ and $\log R = -252.8$, and $m = 71.6$ and $\log R = -250.1$, respectively. It is noteworthy that the parameters R and m are interrelated, as previously suggested by Minnear and Bradt [9]. Indeed, from the data given in Table I, a plot of $-\log R$ against m may be constructed, as shown in Fig. 4 where the values for both types of composite are plotted. A single linear relationship is obtained with a correlation coefficient of $r^2 = 0.972$. Thus, the relation between v and G_I for subcritical crack growth may be determined from a knowledge of either R or m, via Fig. 4 and Equation 7.

TABLE I Subcritical crack growth parameters for interlaminar fracture of the carbon fibre/PEEK composites

Materials	Test no.	Initial crack length (mm)	m	Log R	m_0	Log R_0
APC-2	SCG1	29	104.7	− 332.7	37.9	− 4.17
	SCG2	31	71.1	− 233.9	46.8	− 3.86
	SCG3	35	55.4	− 187.1	51.9	− 3.84
TEXXES	SCG1	29	100.3	− 344.3	63.6	− 2.88
	SCG2	31	72.4	− 252.8	74.1	− 3.15
	SCG3	33	71.6	− 250.1	76.2	− 3.55

4. Discussion

4.1. Results from subcritical crack growth tests

It is clear from comparing Figs 2b and 3b that the APC-2 and the TEXXES composites possess somewhat different R-curves. Hence, to compare more directly the subcritical crack growth in these two materials, the data may be normalized by using the following expression

$$v = R_0 \left(\frac{G_I}{G_{Ic}} \right)^{m_0} \tag{8}$$

The term G_{Ic} is defined here as the "hypothetical" interlaminar fracture energy from the R-curve, which corresponds to the G_I value actually measured during the subcritical crack growth experiments; with the common reference point being the crack length attained at any point during the subcritical crack growth tests. The appropriate value of G_{Ic} was determined by interpolation of the R-curves shown in Figs 2b and 3b, from a knowledge of the crack length throughout the course of the subcritical crack growth test. However, it should be noted that, because the typical increment of subcritical crack growth during the test was only about 1 mm, the value of G_{Ic} is approximately constant for any one test; and is approximately equal to the value of G_{Ic} corresponding to the crack length at the start of the subcritical crack growth test. In Equation 8, the terms R_0 and m_0 are constants. However, the term R_0 has the same dimensions as crack velocity and the parameter m_0 has no dimensions. This is a great advantage in employing Equation 8, rather than Equation 7, because the latter involves the constants R and m which possess somewhat inconvenient dimensions.

Fig. 5 shows values of subcritical crack growth velocity, v, plotted against values of G_I/G_{Ic}, again using logarithmic axes, and the values of m_0 and R_0 are also given in Table I. There are several noteworthy aspects. Firstly, the relationships are linear. Secondly, the results for different values of initial crack length at the start of the tests superimpose quite well for the APC-2 composite, but rather less well for the TEXXES composite. However, for both materials, the value of the initial crack length employed for the subcritical crack tests does somewhat influence the v versus G_I/G_{Ic} relationship. Namely, increasing the crack length (and thereby typically increasing the G_{Ic} value) shifts the crack velocity, v, versus G_I/G_{Ic} curves to slightly higher G_I/G_{Ic} values. These two observations are consistent with results from studies of silicon nitride, which also exhibits a rising R-curve and subcritical crack growth [10]. Thirdly, the slope, m_0, of the linear relationships increases as the crack length increases (i.e. as one goes from test SCG1 to SCG3). The values of m_0 are shown in Table I, and it may be clearly seen that for both types of composite the value of m_0 increases as the crack length increases, and hence as the value of G_{Ic} increases.

Now, assuming that the critical crack growth velocity, v_c, is given when the value at G_I equals G_{Ic},

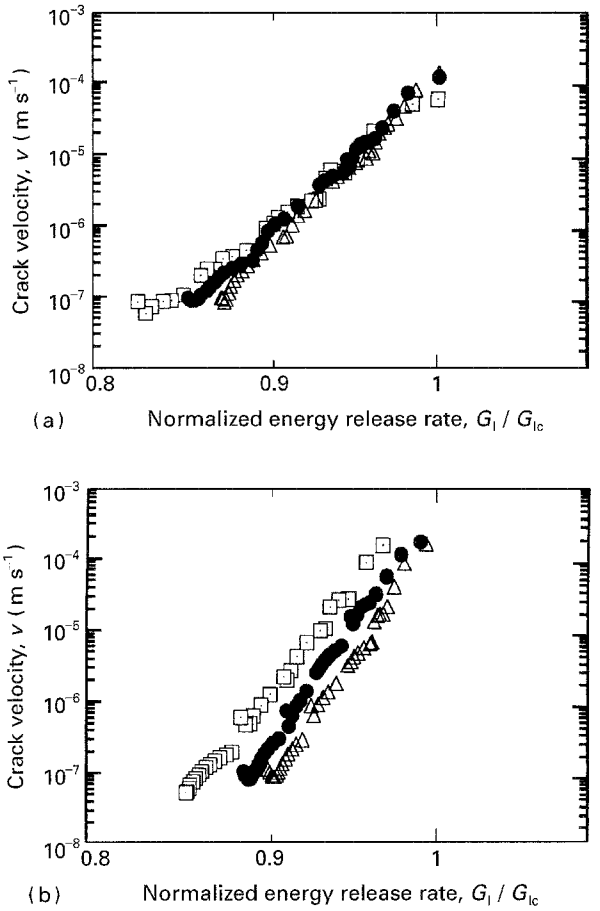

Figure 5 Subcritical crack growth velocity, v, plotted against the normalized crack growth resistance, G_I/G_{Ic}. (a) APC-2 composite; (□) $a = 29$ mm, (●) $a = 31$ mm, (△) $a = 35$ mm. (b) TEXXES composite; (□) $a = 29$ mm, (●) $a = 31$ mm, (△) $a = 33$ mm.

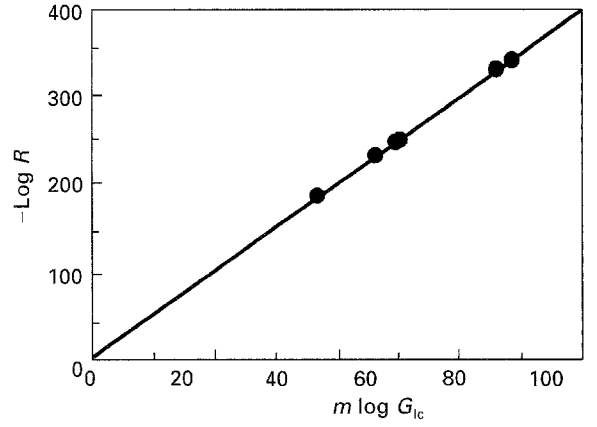

Figure 6 Relationship between the values of $-\log R$ and $m \log G_{Ic}$ for both types of composite. $-\log R = 3.8796 + 0.99930\, m \log G_{Ic}$; $R^2 = 1.000$.

then the following relation may be derived from Equation 7

$$\log R = \log v_c - m \log G_{Ic} \tag{9}$$

Fig. 6 shows a plot of $-\log R$ against $m \log G_{Ic}$, again with results from both types of composite included on the one plot. The excellent linear relationship of $\log R = -3.88 - 0.999\, m \log G_{Ic}$ is obtained, with a correlation coefficient of $r^2 = 1.000$. The value of v_c ascertained from Fig. 6 is 1.32×10^{-4} m s^{-1} and this value may be compared to the average crack velocity

which was measured for stable crack propagation through the composites when tested at the constant crosshead speed of 2 mm min^{-1}. This value was found to be approximately 1×10^{-4} m s^{-1}. Thus, there is excellent agreement between the predicted value of v_c ascertained from the subcritical crack growth experiments, via Fig. 6 and Equation 7, and the experimentally measured value. Further, as commented above, Equation 7 is dimensionally rather unwieldy, and it may be modified to yield Equation 8, by normalizing Equation 7 using the value of G_{Ic}. Obviously, from Equation 8, when the value of G_I equals G_{Ic}, the value of v_c is equivalent to R_0. Hence, the subcritical crack growth experiments also yield a value of R_0 via Equation 8. The average value of R_0, from the results shown in Table I is 2.66×10^{-4} m s^{-1}. Hence, it is clear that Equation 8 may be viewed as an advanced form of expression for subcritical crack growth, because (i) Equation 8 overcomes the problem of unwieldy dimensions for the constants, and (ii) the value of R_0 in Equation 8 is approximately equal to the value of v_c.

4.2. Modelling the fibre bridging

The role of fibre bridging can be explored in more detail by considering that the presence of fibre bridging creates a stress acting across the crack faces, behind the advancing delamination. This stress acts to shield the crack tip from the full effects of the applied stress. Thus, for the subcritical crack growth tests, the strain energy release rate, G_t, at the crack tip may be described by

$$G_t = G_I - G_s \tag{10}$$

where G_s denotes the reduction of the applied strain energy release rate, G_I, which results from the crack-tip shielding effect caused by the presence of the bridging fibres.

Now, the velocity, v, of the subcritical crack growth will be governed by the value of G_t; that is, it will be governed by the strain energy release rate, G_t, actually experienced at the crack tip. Thus, by analogy to Equation 8, in terms of the strain energy release rate, G_t, at the crack tip, the velocity, v, of subcritical crack growth is given by

$$v = R_t \left(\frac{G_t}{G_{tc}} \right)^{m_t} \tag{11}$$

where R_t and m_t are constants and the term, G_{tc} is given by

$$G_{tc} = G_{Ic} - G_{sc} \tag{12}$$

where G_{sc} denotes the reduction of the critical interlaminar fracture energy, G_{Ic}, due to fibre bridging, and the value of G_{Ic} is taken to be the value which is experimentally measured as a function of the length of the propagating crack, a. Hence, the value G_{tc} is that actually experienced at the crack tip during the development of the R-curve.

Next, combining Equations 8 and 10–12, the following relationship between m_0 and m_t may be derived

$$\log\left(\frac{G_t}{G_{tc}}\right) = \frac{m_0}{m_t}\log\left(\frac{G_I}{G_{Ic}}\right) + \frac{1}{m_t}\log\left(\frac{R_0}{R_t}\right) \tag{13}$$

The ratio of m_t to m_0 can be determined from two sets of data, because

$$\frac{m_0}{m_t} = \frac{\log(\alpha_1/\alpha_2)}{\log(\beta_1/\beta_2)} \tag{14}$$

where $\alpha = G_t/G_{tc}$ and $\beta = G_I/G_{Ic}$; and the subscripts 1 and 2 refer to the two sets of data which are needed in order to determine the ratio of m_t to m_0. The relationship between G_s and G_{sc} is not known, although the bridging stress is usually expressed as a function of a crack opening displacement [11, 12]. Therefore, the value of G_s during the subcritical crack growth tests, may be expressed as a function of G_{sc} by

$$G_s = \left(\frac{G_t}{G_{tc}}\right)^u G_{sc} \tag{15}$$

where u is a parameter which describes the dependence of the fibre-bridging stress on the applied stress, couched in terms of G_t and G_{tc}. It is noteworthy that the case of $u = 0$ results in the shielding stress, G_s, during subcritical crack growth being equivalent to the value of G_{sc}; and G_s is therefore essentially a constant and independent of the G_t value. However, if $u = 1$, the value of G_s is proportional to the value of G_t. Fig. 7 shows theoretical plots of the values of m_0/m_t against G_{Ic}/G_{tc} for various values of the parameter u, based on the following expression (see Appendix)

$$\frac{m_0}{m_t} = \frac{\gamma}{u\gamma - u + 1} \tag{16}$$

where $\gamma = G_{Ic}/G_{tc}$, and the value of G_{Ic} is the measured value of the interlaminar fracture energy and the term G_{tc} is the value actually experienced at the crack tip; where $G_{tc} < G_{Ic}$ if fibre bridging occurs. For the case of $u = 0$, then $m_0/m_t = G_{Ic}/G_{tc}$; and for the case of $u = 1$ this leads to $m_0/m_t = 1$.

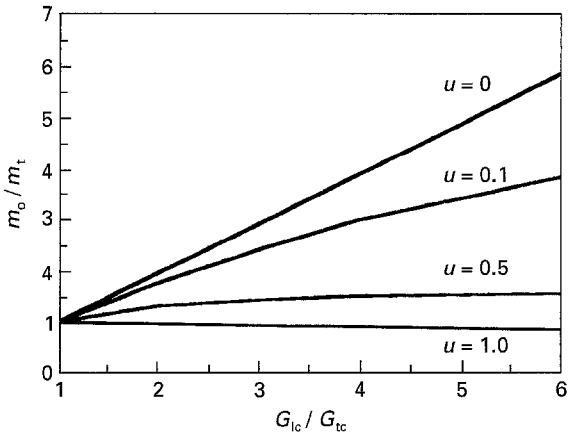

Figure 7 The ratio of m_0/m_t against G_{Ic}/G_{tc}. (Various values of the parameter u have been chosen to describe the function for G_s; see Equation 15.)

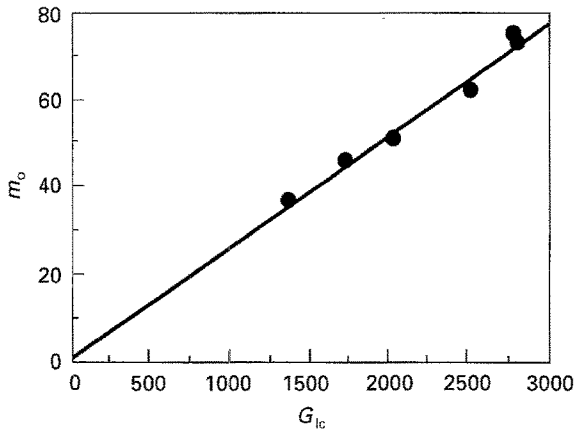

Figure 8 Plots of m_0 against the corresponding value of G_{Ic}. (The value of G_{tc} was assumed to be 1200 J m^{-2}. The value of m_t so obtained is 31.2.)

4.3. Results from the fibre-bridging model

Values of m_0 were obtained from Fig. 5 and are given in Table I. They are shown in Fig. 8 plotted against the corresponding value of G_{Ic} for both the APC-2 and the TEXXES materials. It is found that the results for each material obey the same linear relationship between the values of m_0 and G_{Ic}. Several interesting points arise from this observation. Firstly, by comparison with Fig. 7, this suggests that the value of u is virtually constant and very close to zero for both materials. Secondly, hence, the values of m_t and G_{tc} are independent of the type of composite. Thirdly, both of these observations probably arise because of the similar matrices, fibres, and reinforcement structures in the two types of composite. Fourthly, the value of $u = 0$ means that the value of G_s during subcritical crack growth is equivalent to the value of G_{sc}, and is therefore essentially a constant and independent of the value of G_t. This result suggests that the effect of the bridging zone is relatively constant during subcritical crack growth.

Now the value of G_{tc} may be taken [2, 6] to be 1200 J m^{-2}. This is the typical, minimum, value of G_{Ic} for these composites at the start of the R-curve at the onset of crack growth, when no fibre bridging has yet developed. Hence, from the results shown in Fig. 7 (for $u = 0$) and the values of m_0 given in Table I, the term m_t is found to be a constant with a value of 31.2. However, it should be noted that this m_t value may be somewhat overestimated, because the initiation value of G_{Ic} is difficult to determine accurately, due to the difficulty of observing the exact moment of the onset of delamination growth from the aluminium-foil starter crack. Nevertheless, from Equation 11, it may be seen that, when the subcritical crack growth is expressed in terms of the strain energy release rate, G_t, actually experienced at the crack tip, the power-law index is a constant, and independent of the exact type of starting prepreg and the initial crack length used for the tests.

As discussed above, the mode I interlaminar fracture behaviour of the APC-2 and TEXXES composites is basically similar, as reflected by the values of m_t and G_{tc} being similar for both types of composite. The only major difference being the tendency for the TEXXES material to exhibit slip–stick crack growth when loaded at a constant rate of displacement, and it is suggested that this may result from fibre-bridging effects. In the APC-2 material, stable fracture is typically observed and a clear rising R-curve is recorded. In contrast, the TEXXES material is apt to exhibit slip–stick behaviour and the R-curve behaviour is therefore more complex and tends to be less reproducible. It is suggested that this arises from fibre-bridging effects. Namely, that the APC-2 composite develops a uniform fibre-bridging zone, whilst that in the TEXXES composite is far less uniform in any given specimen and less reproducible. This implies that the distribution of the traction stress behind the advancing delamination in the APC-2 material is relatively uniform over the range of fibre-bridging zone, whilst the stress distribution in the TEXXES material fluctuates. These differences in the fibre-bridging effect would be expected from the different structures of the two types of composite prepreg. The APC-2 material is produced by hot-pressing the common type of prepreg sheets and misalignment of carbon fibres in the finished sheet is relatively minor. The resulting bridging behind the crack tip, and crack-tip splitting, therefore seem to occur in a relatively regular way. In contrast, the TEXXES materials are made from prepregs which consist of mixed textiles of carbon and PEEK fibres and in the hot-pressed sheet misalignment of carbon fibres is far more common. This may cause a greater variation in the development of the fibre-bridging zone, and may therefore be responsible for the tendency for this composite to exhibit slip–stick crack growth, and possess a more complex R-curve.

5. Conclusion

Subcritical crack growth behaviour has been evaluated in composite laminates, based on uniaxial carbon fibres in poly(ether-ether ketone) (PEEK) matrices. Double cantilever beam (DCB) specimens have been employed to give mode I loading, and it has been shown that the materials exhibit a rising R-curve, i.e. the value of the interlaminar fracture energy, G_{Ic}, increased as the crack propagated through the specimens. Secondly, with a knowledge of the R-curve, another specimen was loaded at constant crosshead speed of 2 mm min^{-1}, and again the crack was allowed to propagate whilst the load and displacement were recorded. However, in this test the crosshead was occasionally stopped and the displacement held constant. During the period the displacement was held constant the relaxation of the applied load was recorded as a function of time, and the position of the crack was also monitored. Subcritical crack growth was observed to occur during this period, and values of the crack velocity, v, have been obtained as a function of the corresponding applied strain energy release rate, G_I. Owing to the presence of the R-curve, these data have been measured at various stages during the development of the R-curve.

The relationships between v and G_I have been successfully modelled using a simple power law. However, a normalized expression of the form $v = R_0(G_I/G_{Ic})^{m_0}$ has been proposed, where the term G_{Ic} is defined here as the "hypothetical" interlaminar fracture energy from the R-curve, which corresponds to the G_I value actually measured during the subcritical crack growth experiments; with the common reference point being the crack length attained at any point during the subcritical crack growth tests. The appropriate value of G_{Ic} was determined by interpolation of the R-curves, from a knowledge of the crack length throughout the course of the subcritical crack growth test. The terms R_0 and m_0 are constants. The above expression has been shown to be more useful than the simple power law for interpreting the subcritical crack growth data, because (i) the dimensions for the constants m_0 and R_0 are no longer unwieldy, and (ii) the value of R_0 is equal to the value of the critical crack velocity, v_c, for interlaminar failure when $G_I = G_{Ic}$.

Finally, the R-curve behaviour has been considered to be most likely caused by the fibre bridging, which develops behind the crack tip as the delamination propagates through the specimen. Fibre bridging allows stress to be transferred across the crack faces, behind the advancing crack tip, and so results in a "shielding" of the stress field at the crack tip from the applied stress. Therefore, the above relationship between the velocity, v, of subcritical crack growth and the corresponding value of G_I has been further refined and modelled to account for the presence of fibre bridging. The model defines a term G_s which denotes the reduction of the applied strain energy release rate, G_I, during subcritical crack growth; this reduction resulting from the crack tip being shielded due to the presence of the bridging fibres. The value of G_s during subcritical crack growth has been found to be a constant, and this suggests that the effect of the bridging zone behind the crack tip was relatively constant during the process of subcritical crack growth. Thus, when the subcritical crack growth is expressed in terms of the strain-energy release rate, G_t, actually experienced at the crack tip, the power-law index in the equation which describes the relation between v and G_t is a constant, and is also independent of the exact type of prepreg and the initial crack length used for the tests.

Acknowledgement

The authors would like to acknowledge the financial support for Mr Dyson from the Nissan Motor Co. Ltd.

Appendix

Equation 16 may be derived as follows. Equations 10, 12 and 15 are

$$G_t = G_I - G_s \tag{10}$$

$$G_{tc} = G_{Ic} - G_{sc} \tag{12}$$

$$G_s = \left(\frac{G_t}{G_{tc}}\right)^u G_{sc} \tag{15}$$

If $\alpha = G_t/G_{tc}$ and $\beta = G_I/G_{Ic}$ and $\gamma = G_{Ic}/G_{tc}$, then the term, β, may be expressed as

$$\beta = \frac{\alpha}{\gamma} + \alpha^u\left(1 - \frac{1}{\gamma}\right) \tag{A1}$$

Now, if we let $\alpha_1 = 1 - \xi_1$ and $\alpha_2 = 1 - \xi_2$, where $0 < \xi_1 < \xi_2 \ll 1$, then $\log(\alpha_1/\alpha_2) = \log(1 - \xi_1) - \log(1 - \xi_2) = \xi_2 - \xi_1$.

Similarly, because $\beta_1 = 1 - \xi_1(u\gamma - u + 1)/\gamma$ and $\beta_2 = 1 - \xi_2(u\gamma - u + 1)/\gamma$, then $\log(\beta_1/\beta_2) = \log[1 - \xi_1(u\gamma - u + 1)/\gamma] - \log[1 - \xi_2(u\gamma - u + 1)/\gamma] = (\xi_2 - \xi_1)(u\gamma - u + 1)/\gamma$.

Now, Equation 14 is

$$\frac{m_0}{m_t} = \frac{\log(\alpha_1/\alpha_2)}{\log(\beta_1/\beta_2)} \tag{14}$$

and we can therefore express this equation as a function of u and γ to give

$$\frac{m_0}{m_t} = \frac{\gamma}{u\gamma - u + 1} \tag{16}$$

References

1. W. M. JORDAN, W. L. BRADLEY and R. J. MOULTON, *J. Compos. Mater.* **23** (1989) 923.
2. S. HASHEMI, A. J. KINLOCH and J. G. WILLIAMS, *ibid.* **24** (1990) 918.
3. *Idem, Compos. Sci. Technol* **37** (1990) 429.
4. S. M. SPEARING and A. G. EVANS, *Acta. Metall. Mater.* **40** (1992) 2191.
5. A. OKADA, I. N. DYSON and A. J. KINLOCH, *J. Mater. Sci. Lett.* **12** (1993) 1815.
6. I. N. DYSON, A. J. KINLOCH and A. OKADA, *Composites*, **25** (1994) 189.
7. S. HASHEMI, A. J. KINLOCH and J. G. WILLIAMS, *Proc. R. Soc. Lond. A* **427** (1990) 173.
8. A. J. RUSSELL, in ASTM STP 1110 (American Society for Testing and Materials, Philadelphia, PA, 1991) p. 226.
9. W. P. MINNEAR and R. C. BRADT, *J. Am. Ceram. Soc.* **58** (1975) 345.
10. A. OKADA, N. HIROSAKI and M. YOSHIMURA, *ibid.* **73** (1990) 2095.
11. Y. M. MAI and B. R. LAWN, *ibid.* **70** (1987) 289.
12. C. W. LI, D. J. LEE and S. C. LUI, *ibid.* **75** (1992) 1777.

Received 10 March
and accepted 4 November 1994